Title
BUOYANCY-DRIVEN CONVECTION IN A RECTANGULAR ENCLOSURE: EXPERIMENTAL RESULTS AND NUMERICAL CALCULATIONS

Author
Bauman, Fred

Publication Date
1980-07-01

Lawrence Berkeley Laboratory
UNIVERSITY OF CALIFORNIA

ENERGY & ENVIRONMENT DIVISION

Presented at the American Society of Mechanical Engineers Conference on Heat Transfer in Passive Solar Systems, Orlando, FL, July 27-30, 1980

BUOYANCY-DRIVEN CONVECTION IN A RECTANGULAR ENCLOSURE: EXPERIMENTAL RESULTS AND NUMERICAL CALCULATIONS

Fred Bauman, Ashok Gadgil, Ronald Kammerud, and Ralph Greif

July 1980

Prepared for the U.S. Department of Energy under Contract W-7405-ENG-48

LBL-10257
July 1980

BUOYANCY-DRIVEN CONVECTION IN A RECTANGULAR ENCLOSURE: EXPERIMENTAL RESULTS AND NUMERCIAL CALCULATIONS

Fred Bauman, Ashok Gadgil, Ronald Kammerud, and Ralph Greif*
Passive Solar Analysis and Design Group
Lawrence Berkeley Laboratory
Berkeley, California 94720

ABSTRACT

Within the building sciences, little attention has been given to buoyancy-driven convection in room geometries at the large Rayleigh numbers which typify full-scale structures. Natural convective heat transfer processes are fundamental to the operation of many passive solar systems. In order to fully understand system performance and to allow design optimization, the characteristics of this heat transfer process must be examined from first principles. For this reason, an investigation of two- and three-dimensional buoyancy-driven convection in rectangular enclosures at Rayleigh numbers approaching 10^{10} has been initiated at Lawrence Berkeley Laboratory. This report will focus on the technical details of the experimental analysis performed to date and on the comparison of the numerical results with published data. Initial results are also presented from the application of the convection analysis computer program to simulate convective heat transfer arising from a few representative room surface temperature distributions.

I. INTRODUCTION

Natural convection heat transfer processes are expected to play a fundamental role in the operation of many passive solar systems. Recent research results (1) have shown that convective heat exchange can have a surprisingly large magnitude in passive systems in which conduction had been expected to be the dominant process. This reference indicates that convection between the attached greenhouse and occupied space in the Balcomb house in Santa Fe, New Mexico, is nearly an order of magnitude larger than conduction through the solar collecting adobe wall separating the two spaces. The implication of this finding is clear: natural convection can be a significant component in the coupling of thermal zones within a building. This is especially important in passive solar systems where successful operation relies upon proper utilization of the basic heat transfer processes--radiation, conduction and convection--rather than upon mechanically assisted heat transfer.

Beyond the general problem described above, natural convection is utilized in other, more specific passive solar systems. Among these are:

- thermocirculation in storage wall channels;
- convection in double-envelope configurations;
- stack effect ventilation in multi-story atria;
- solar chimneys;
- natural convection air collectors connected to rock storage units.

In order to understand the thermal operation of these systems and to provide relevant building design guidelines, improved understanding of natural convection processes is necessary.

Past convection research (see Appendix 1) has dealt primarily with geometric configurations which do not typify buildings and/or with forced convection; as a result, these studies are of limited application to passive solar research. More recently there has been renewed interest in natural convection within the building sciences. Thermocirculation has been studied experimentally by Hocevar and Casperson (2) and analytically by Akbari and Borgers (3,4). Similitude and/or full-scale experimental investigations of convective heat transfer within and

---

*Department of Mechanical Engineering, University of California, Berkeley, California 94720.

This work was supported by the Passive and Hybrid Systems Branch, Systems Development Division, Office of Solar Applications, U.S. Department of Energy, under Contract No. W-7405-ENG-48.

between thermal zones have been reported by Honma (5), researchers at MIT (6), Los Alamos Scientific Laboratory (7,8), and by one of the present authors (9); limited preliminary numerical results from the present study have been presented (10). To date there has been little analytic work addressing the general problem of natural convection in either single or multi-room geometries.

The objective of the work reported here was to develop and validate computer codes for analysis of buoyancy-driven, recirculating laminar flow in two and three dimensions. In order to validate these codes, a small-scale natural convection experiment has been performed.

Appendix 1 describes a general problem in buoyancy-driven convection in rectangular enclosures. The prototypical problem presented there is representative of several passive solar configurations; for example, it is analogous to an unvented Trombe wall delivering heat to an occupied space or to a direct solar gain system losing heat through the south glazing. Representative values of the dimensionless parameters describing the convection process for a rectangular room twice as long (5.5 m) as it is high (2.75 m), filled with air at 21°C, and with at least a 1°C temperature difference between vertical walls of at least 1°C are:

$$A = 0.5$$

$$Pr = 0.71$$

$$Ra_L = Gr_L Pr \geq 1 \times 10^{10}$$

This range of Ra_L implies that convective flow within buildings can be either laminar or turbulent in nature, depending on the specific temperature distributions on the boundary surfaces and the geometry of the enclosure.

Section II below describes the experiment and summarizes the results. Section III outlines the numerical analysis and presents comparisons of the results with several experiments; these validations have used data cited in the literature and the results from the experiment described in Section II. Section IV presents a few results that have been obtained by applying the computer program to specific passive solar configurations and briefly outlines the future directions of the natural convection studies at Lawrence Berkeley Laboratory.

II. NATURAL CONVECTION EXPERIMENT

A. Experimental Overview

The experimental apparatus is shown schematically in Fig. 1; it was scaled to table-top size and utilized water as the working fluid. The apparatus was designed to measure natural convection within a single zone and between two geometrically identical zones separated by a partition. Most of the results presented here considered the single enclosure configuration, in which the experiment covered the following range of parameters:

$$A = 0.5$$

$$2.6 \leq Pr \leq 6.8$$

$$1.6 \times 10^9 \leq Ra_L = Gr_L Pr \leq 5.4 \times 10^{10}$$

The opacity of water to thermal radiation makes the data from this experiment especially appropriate for validation of the convection analysis code.* In addition, the use of water was convenient because it allowed representative Ra values to be obtained in a small-scale apparatus; however, strict similarity to full-scale rooms could not be obtained due to Prandtl number differences. Raithby (11) has pointed out that the heat transfer processes are insensitive to Prandtl number for $Pr \geq 5$. This partially covers the range of Prandtl numbers encountered in the present experiment, and implies possible limitations to the use of this data in the development of correlations representing enclosures using air as the working fluid [Pr(air) = 0.7]. Thus, while the magnitude of Nusselt numbers measured in this experiment are not accurate for air, the general fluid behavior and parametric relationship can be expected to be similar.

B. Apparatus

A rectangular enclosure with inside dimensions 12.7 cm x 25.4 cm x 76.2 cm was fabricated from 1.3 cm clear plexiglas, except for the two vertical opposing side walls (12.7 cm x 76.2 cm), which were 0.5 cm cold-rolled copper sheets. The 76.2 cm length of the enclosure was designed to

*The maximum contribution of thermal radiation to the measured Nusselt number has been calculated to be less than 2% for the range of Rayleigh numbers covered by the experiment.

minimize the relative end effects and create a two-dimensional problem. For studying the two-zone problem, a partition (0.6 cm plexiglas) could be lowered from the top midway between the two copper plates, thus forming a two-dimensional opening between thermal zones. A cross-sectional view of the test enclosure is shown in Fig. 2.

Constant heat input was provided by six thermofoil heaters (maximum power = 3.1 W/cm^2) attached to the outside surface of one copper plate. Heat was removed through the opposite copper plate, 25.4 cm away, by running cool tap water (15^oC) through four horizontal lengths of 1.0 cm O.D. cold-rolled copper tubing glued to the outside surface with a high conductivity cement. The entire enclosure was covered with a 10 mil layer of polyethylene sheeting, to reduce convective losses, and a shell of 5.1 cm polystyrofoam insulation board. The closed cell construction of the styrofoam acted as an additional vapor barrier.

All temperature measurements were made with calibrated copper-constantan thermocouples, which were read on a standard 100 mV potentiometer to a total accuracy of $\pm$ 0.6^oC. Figure 3 shows a schematic of the thermocouple locations. Ten thermocouples were embedded 1.5 mm beneath the inside surface of each copper plate to monitor temperature variations over the heat transfer surface. Five thermocouples were positioned along the bottom edge of the partition as well as along the bottom of the enclosure directly beneath the partition to measure top and bottom surface temperature at the centerline (single enclosure) or central opening (two-zone enclosure). A vertical array of thermocouples was placed beneath the midpoint of the partition to measure the centerline (central opening) vertical temperature profile in the fluid. Holes in the plexiglas ceiling allowed thermocouple probes to be lowered to desired depths at various locations in the enclosure.

The experimental procedures are described in Appendix 2.

C. Results and Discussion

The dimensionless temperature, = $(T - T_{avg})/\Delta T^*$, measured along the vertical centerline of the enclosure (at $y/L = 0.5$), when plotted as a function of the dimensionless height x/H, displayed a constant slope in the central region.* This indicates a rather large inactive core, in which only conduction in the vertical direction is significant. The non-zero slopes of the profiles at $x/H = 0.0$ and 1.0 also demonstrate that there is heat loss through both the top and bottom surfaces of the enclosure. Heat losses through the insulated surfaces (top, bottom, and two ends), as measured by the difference between heat input and output, ranged from 7-18% (calculated for $\Delta T_{CW} > 5.6^oC$).

The heat transfer data is presented in the form of $\log_{10}(Nu_{L_{IN}})$ vs. $\log_{10}(Ra_L)$ in Fig. 4. Results of the studies by Raithby, Hollands, and Unny (11) and by MacGregor and Emery (12) are also shown in the figure; results from the experiment appear to be consistent with both of these studies. As expected, the smaller aspect ratio of this experiment yields higher average Nusselt numbers in the laminar regime compared to the predictions of Raithby et al. for A = 5. Although Raithby's analysis does not claim validity for aspect ratios less than five, the measured temperature profiles in the core region of the enclosure in the present study appear to support an extension of his results to lower aspect ratios. This extrapolation is shown in Fig. 4; it is in agreement with the data from the present experiment to within the experimental error. The retarding influence of the relatively larger horizontal surface areas in an enclosure of aspect ratio 0.5 (rather than Raithby's 5.0), as well as the known heat losses through these horizontal surfaces, may make a large contribution to the observed difference.

Isothermal vertical walls were assumed in the study by Raithby et al. MacGregor and Emery, while maintaining a constant cool wall temperature, imposed a constant heat flux condition on the heated wall. As noted by the authors, this constant heat flux boundary condition will result in a portion of the fluid being hotter than the average heated wall temperature, and in effect, will increase the predicted net heat transfer rate. In the present study, vertical boundary conditions were not perfectly isothermal; the experimental calculations are based on single average temperatures.

A plot of the data obtained in preliminary tests using the two-zone configuration is presented in Fig. 5. For these cases the convective heat transfer rate was calculated by measuring the conductive heat transfer through the central partition (Q_P) and subtracting this amount from the heat input (Q_{IN}) and heat output (Q_{OUT}). This correction resulted in a redefinition of the Nusselt number for the two-zone problem:

*These profiles are shown in Figs. 13 and 15 where comparison of this data to the predictions of the convection analysis code are discussed.

$$\overline{Nu}_{L_{IN}} = \frac{(Q_{IN} - Q_P)L}{kA_P\Delta T}, \quad \overline{Nu}_{L_{OUT}} = \frac{(Q_{OUT} - Q_P)L}{kA_P\Delta T}$$

Data was collected for three different opening heights (H_0). The results demonstrate the expected thermal behavior of decreasing convective heat transfer rates with decreasing opening heights. When the opening height H_0/H was reduced from 1.0 (full open) to 0.55, the measured Nusselt numbers dropped by about 25% at $Ra_L = 3.7 \times 10^{10}$. At lower values of Ra_L, a relatively smaller decrease in the Nusselt number was observed. The measured temperature profiles in the central opening indicated that most of the heat transfer from the warm zone to the cool zone was confined to a small region at the top of the opening. This result is in qualitative agreement with the results of Weber et al. (5). The opposite horizontal motion of fluid from the cool zone to the warm zone was contained in a thicker layer along the enclosure bottom.

III. NUMERICAL ANALYSIS

A. Description

As pointed out in Appendix I, there has been little published numerical work on natural/buoyant convection at Rayleigh numbers in excess of 10^7, where relatively large fluid velocities are encountered. If the popular Central Difference Scheme (CDS) is used for casting the Navier-Stokes equations into finite difference form, these large velocities necessitate an impracticably fine mesh size for numerical stability of the solution. The Upstream Difference Scheme (UDS), which takes into account the overwhelming effect of convection (vis à vis conduction/diffusion at large fluid velocities) cannot be used to simulate recirculating flow since the fluid velocities are not large everywhere and the direction of the fluid velocity is not known at all points before solving the problem.

In recent years Spalding (13) has proposed a differencing scheme that switches between the CDS and UDS depending on the relative magnitudes of (local) convection and (local) conduction/diffusion. Thus, grid spacings can be chosen to be relatively coarse without seriously compromising accuracy (14).

A computer program was developed based on this differencing scheme to solve the coupled two-dimensional Navier-Stokes equations with the Boussinesq approximation. The Alternating Direct Implicit scheme (ADI) was used for solving the difference equations (15). The resulting program structure was similar to that described in detail by Patankar (16).

The mesh sizes used in all the results presented in this paper were relatively coarse (the finest mesh size was 17x20). The grid lines were distributed evenly throughout the interior of the fluid volume with a concentration of grid lines near the enclosure boundaries; this allows the numerical solution to account for the sharp changes in flow properties associated with a developed boundary layer. For this purpose, it was found to be adequate to position three grid lines parallel to and adjacent to each enclosure surface. The computer program, presently limited to laminar flow, can simulate enclosure flows driven by buoyancy, and/or pressure, and/or velocity. For more details, see Ref. (17). The comparisons of the calculated results of the above numerical scheme with various published numerical and experimental results are described below.

B. Comparison at Rayleigh Numbers Near 1.0×10^5

de Vahl Davis (18) used an 11x11 grid to solve the Navier-Stokes equations for buoyancy driven fluid flow inside a two-dimensional square cavity. The two vertical walls of the cavity were maintained at constant, but different temperatures; the ceiling and the floor of the cavity had a linear surface temperature profile. For this problem, the boundary layer regime starts for $Ra_L > 10^4$. Figures 6, 7, and 8 compare the numerical results with those of de Vahl Davis, for three different Rayleigh numbers.

de Vahl Davis used an evenly-spaced grid and a forward differencing procedure to calculate the local Nusselt numbers at the wall. The boundaries of his temperature grid coincided with the surfaces of the cavity, so the nearest temperature node in the direction normal to the surface was at a distance equal to 10% of the cavity dimension. In contrast, the grid system used here allowed evaluation of the temperature gradient at the boundary without using a forward differencing procedure. These results were calculated using a 15x15 grid size.

Due to his choice of the grid scheme, de Vahl Davis calculated the local Nusselt number at the top and bottom of the cold wall to be identically equal to 1.0 (see Figs. 6 to 8). This resulted from locating the temperature node exactly at the corner of the cavity, the nearest temperature node along the surface again being at a distance of 10% of the cavity dimension. The grid scheme used in the present analysis does not have this limitation; for this reason the local Nusselt numbers at the two ends of the wall differ from 1.0.

In these calculations, two grid lines were outside the physical boundary, two more grid lines were in the boundary layer; the grid cell size inside the volume of the cavity was therefore the same as for de Vahl Davis (1/10 x 1/10). The computation for each run took 31 seconds to reach residues of 10^{-7} for velocity fields.

C. Comparisons at Higher Rayleigh Numbers

A quantity of special interest in this problem is the Nusselt number. In Fig. 9, the average Nusselt number, defined here as:

$$\overline{Nu}_L = \frac{1}{T_H - T_C} \int_0^H \frac{\partial T}{\partial y}\, dx$$

as calculated by the convection analysis code, is plotted as a function of Rayleigh number. This figure also shows relevant results from various other numerical and experimental studies (18-23). The agreement is quantitatively acceptable. All of the present results were calculated using a 17x17 grid similar that described above. For Rayleigh numbers of 10^7 or less, the code converged in 20 seconds on the CDC-7600 at LBL. The execution time for higher values of the Rayleigh number was 40 seconds.

D. Comparison with a Full-Scale Three-Dimensional Experiment

In 1978, Ruberg reported a full-scale experiment performed at the Massachusetts Institute of Technology; the experiment is schematically depicted in Fig. 10. Temperature distribution inside the enclosure was measured in plane AA by means of an array of thermistors mounted on a rail-mounted, movable boom. Videotapes of the flow induced inside the enclosure were also made using smoke and soap bubbles as tracers. The videotapes clearly demonstrated that the flow (at Rayleigh number of 1.0×10^{10} based on enclosure height) was not yet turbulent, but showed oscillations typical of the transition regime. Unfortunately, no temperature measurements of surfaces other than the heater-plate and window were made; for the present analysis, these temperatures have been estimated using available data.

Ruberg's measurements of air temperature were made in a way that could not exclude the effects of radiation. In particular, these effects are expected to bias the measured air temperatures directly above the heater plate towards higher values.

The isotherms generated for three sets of measurements of air temperatures in the measurement plane are shown in Fig. 11; the isotherms predicted by the present numerical scheme applied to three dimensions are shown in Fig. 12. The agreement between the numerically predicted and experimentally measured isotherms is qualitatively satisfactory. In light of the limitations described above, a disagreement of 33% between numerically predicted and experimentally estimated convective Nusselt numbers (180 vs. 270) is seen to be acceptable.

E. Comparison with Present Experimental Data

In order to simulate the experiment described in Section III, modifications were made to the computer program to account for the temperature-dependent variations of the Prandtl number, (Pr), and the coefficient of thermal expansion, (β), of the working fluid. The combined effect of these two parameters tends to enhance the effect of the temperature difference on the flow; a stronger buoyant force and a weaker viscous force will be encountered in the hotter fluid. Sensitivity runs of the computer program demonstrated an increase of up to 10% in the Nusselt numbers when Pr and β were allowed to vary, as opposed to fixing them at their average values. A typical computer run for this problem on the CDC-7600 at LBL required 57 seconds of execution time.

The accuracy of the calculated numerical solution is largely dependent on an accurate specification of the two-dimensional surface temperature distribution. As described earlier, both of the vertical copper plates in the experiment were well monitored. However, during the experimental design, it was not anticipated that horizontal surface temperatures would also be a crucial measurement. As a result, a best estimate of the temperature profiles on both horizontal surfaces had to be made from the available data.

Comparisons were made at two values of Ra_L spanning the range of experimental results. Vertical and horizontal centerline temperature profiles for $Ra_L = 2.4 \times 10^9$ are shown in Figs. 13 and 14. The agreement is excellent, particularly in the numerical predictions of the degree and extent of the central core stratification. The reasonable agreement of Nusselt numbers (see Table 1) and temperature profiles seems to indicate that the program is addressing the fundamental characteristics of the flow successfully at this Rayleigh number (2.4×10^9).

Comparisons at the higher Rayleigh number ($Ra_L = 4.7 \times 10^{10}$) are presented for the Nusselt number in Table 1, and the vertical and horizontal centerline temperature profiles in Figs. 15 and 16. At this value of Ra_L two numerical analyses were performed (Runs 2a and 2b). Run 2a represented an attempt to duplicate experimental surface temperatures. In run 2b, the heated and top surfaces were held constant at the measured average hot plate temperature (T_H) and the cooled and bottom surfaces were held constant at the measured average cold plate temperature (T_C). This was motivated by the experimental observation that the measured centerline temperatures of the top and bottom horizontal surfaces were very close (within 4%) to the measured average temperatures of the hot and cold vertical surfaces, respectively. In this way the attempt was made to quantify the effect of the uncertainty in the estimation of the horizontal surface temperatures. on the numerical results.

As seen in Table 1, the numerically predicted $Nu_{L_{IN}}$ is increased by only 16% in going from run 2a to 2b. While this result is certainly encouraging, it also demonstrates the degree of sensitivity of the predicted Nusselt number to a detailed specification of the surface temperatures. The numerical vertical centerline temperatures shown in Fig. 15 exhibit a shift to smaller temperature gradients in the central core region associated with an increased gradient near the horizontal surfaces. The potential for turbulent or at least transitional flow at this value of Ra_L could contribute to the noted differences between experimental and numerical results. The possibility also exists that the surface temperatures immediately upstream from the centerline region have a significant effect on the magnitude of the calculated temperature profile at the centerline. Work is presently under way to investigate the sensitivity of the vertical centerline temperature gradient to such surface temperature specifications.

IV. APPLICATIONS AND FUTURE WORK

The numerical analysis program was used to investigate convective heat transfer processes in a single thermal zone in a building. In particular, the validity of the assumption (made by most existing building energy analysis programs) that the convective heat transfer coefficients for interior surfaces are constant,* is being tested.

The calculated convective heat fluxes from the surfaces of a two-dimensional room are displayed in Fig. 17 for three different specifications of surface temperature distributions on the cool vertical wall; the average temperature of the wall was maintained at 15.6°C in all three cases. The average (convective) Nusselt number for each of the six interior surfaces of a three-dimensional cubical room are shown in Fig. 18, again for three different surface temperature configurations. As indicated in both of these figures, the numerical scheme predicted substantial changes (up to 50%) in the heat flux from the various surfaces resulting from relatively small changes in the surface temperature distributions. The effect of these changes on building load profiles and on internal air temperatures are currently being investigated.

In addition to more extensive validations and applications of the convection analysis program, efforts are also under way to refine the three-dimensional numerical model. The inclusion of a model of buoyancy driven turbulence is under consideraton, allowing a wider range of applicability of the computer program.

Work is now under way on an improved experimental apparatus which will (1) have the capability of controlling the heat flux distribution on the heated wall in an effort to produce an isothermal wall (or constant heat flux wall); (2) have an improved cooling system with a grooved manifold milled directly into the backside of the cooled plate; (3) be instrumented more completely with smaller and more precise thermocouples and thermistors; (4) have improved insulation to reduce uncontrolled shell losses; and (5) be capable of investigating single and two-zone enclosures with aspect ratios of

*Some of the existing programs include a convection coefficient dependence on heat flow direction for non-vertical surfaces. These dependences typically do not include explicit temperature or geometry dependence.

$0.1 \leq A \leq 0.5$.

The primary emphasis in this second series of experiments will be to perform a thorough examination of convective heat transfer between thermal zones. The results from these experiments will provide complete data for comparison to and validation of the numerical analysis for single and two-zone enclosure configurations. Extensive experimental work on the two-zone enclosure problem is needed to (1) study the functional dependence of the convective heat transfer rate on the central opening height and width; (2) determine the characteristic temperature difference between thermal zones; (3) perform flow visualization and fluid velocity studies; and (4) determine the applicability of the model to full-scale buildings.

V. SUMMARY AND CONCLUSIONS

Buoyancy driven convective heat transfer in the range $1.6 \times 10^9 \leq Ra_L \leq 5.4 \times 10^{10}$ has been experimentally investigated in a small, two-dimensional rectangular enclosure with an apsect ratio of 0.5 using water as the working fluid. Preliminary results are also presented for natural convection in a two-zone enclosure. The heat transfer results obtained in this study for the single zone configuration compare well with previous studies. Direct scaling of these results to a full-scale room with air is not possible due to Prandtl number differences. The experimental data are seen to be useful in validating analytic techniques and in planning future full-scale experimental studies.

The results of the numerical simulation of buoyancy-driven convection reported here have been compared with both experimental and numerical results of other investigators, covering the range of $10^4 \leq Ra_L \leq 10^9$. The agreement is excellent. The numerical prediction of buoyancy driven flow (at $Ra_L = 10^{10}$) in a three-dimensional full-scale enclosure is shown to be satisfactory within the limitations of existing data. A detailed comparison of numerically predicted Nusselt numbers and temperature profiles with the results of the experiment reported here exhibits good agreement. The numerical technique appears to be successful in simulating buoyancy driven flows in rectangular enclosures for $Ra_L < 10^{10}$. The computer program is used to simulate the convective flow resulting from a few representative surface temperature distributions in a full-scale room. It was found that the assumption (made by most existing state-of-the-art building energy analysis programs) of constant convective heat transfer coefficients for various interior surfaces may not be warranted.

NOMENCLATURE

A	aspect ratio, H/L
A_p	area of heat transfer plate, m^2
g	acceleration of gravity, m/sec^2
Gr_L, Gr_H	Grashof number, $g\beta\Delta TL^3/\nu^2$, $g\beta\Delta TH^3/\nu^2$
H	height of enclosure, m
H_0	height of central opening
k	thermal conductivity, W/m^oC
L	length of enclosure, m
$\overline{Nu}_L$, $\overline{Nu}_{L_{IN}}$, $\overline{Nu}_{L_{OUT}}$	average Nusselt number, $\frac{L}{\Delta T}\int_0^1 \frac{\partial T}{\partial X}$, $\frac{q_{IN}L}{\Delta Tk}$
$\overline{\overline{Nu}}_{L_{IN}}$, $\overline{\overline{Nu}}_{L_{OUT}}$	average Nusselt number (2-zone enclosure) $\frac{(Q_{IN} - Q_p)L}{kA_p\Delta T}$, $\frac{(Q_{OUT} - Q_p)L}{kA_p\Delta T}$
Pe	Péclet number, VL/Γ
Pr	Prandtl number, ν/α
q_{IN}	average heat flux input, W/m^2
q_{OUT}	average heat flux output, W/m^2
q_{var}	variation in vertical plate surface heat flux, W/m^2
Q_{IN}	heat input, W
Q_{OUT}	heat output, W
Q_p	rate of heat conduction through central partition, W
Ra_L, Ra_H	Rayleigh number, $\frac{g\beta\Delta TL^3Pr}{\nu^2}$ $\frac{g\beta\Delta TH^3Pr}{\nu^2}$
t	thickness of central partition, m
T	temperature, ^oC

T_{avg} average temperature, $= (T_H + T_C)/2$, ^oC

T_H average temperature of heated plate, ^oC

T_C average temperature of cooled plate, ^oC

T_{IN} cooling water inlet temperature, ^oC

T_{OUT} cooling water outlet temperature, ^oC

T_{var} variation in vertical plate temperature, ^oC

ΔT vertical plate temperature differential, $T_H - T_C$, ^oC

ΔT_{CW} cooling water temperature differential, $T_{OUT} - T_{IN}$, ^oC

ΔT^* (maximum heated plate temperature) - (minimum cooled plate temperature), ^oC

V local fluid velocity, m/sec

x direction parallel to the height of the enclosure, m (Fig. 1)

y direction parallel to the length of the enclosure, m (Fig. 1)

α thermal diffusivity, m^2/sec

β coefficient of cubical thermal expansion, $1/^oC$

Γ diffusivity ($=\alpha$ for energy, $=\nu$ for momentum)

ρ density, kg/m^3

ν kinematic viscosity, m^2/sec

θ dimensionless temperature, $(T-T_{avg})/\Delta T^*$

REFERENCES

(1) Balcomb, J.D., Hedstrom, J.D., Moore, S.W., "Performance Data Evaluation of the Balcomb Solar Home," LASL Report No. LA-UR-79-2659 (1979).

(2) Hocevar, C.J. and Casperson, R.L., "Thermocirculation Data and Instantaneous Efficiencies for Trombe Walls," in Proceedings, 4th Nat'l Passive Solar Conf., Kansas City, Mo., 3-5 October 1979.

(3) Akbari, H. and Borgers, T.R., "Free Convective Laminar Flow Within the Trombe Wall Channel," Solar Energy, 22, 165-174 (1979).

(4) Borgers, T.R., Akbari, H. and Kammerud, R.C., "Free Convective Turbulent Flow Within The Trombe Wall Channel," Lawrence Berkeley Laboratory Report LBL-8323 (April 1979).

(5) Honma, H. "Ventilation of Dwellings and Its Disturbances," Ph.D. Thesis, Royal Institute of Technology, Stockholm, Sweden (1975).

(6) Ruberg, K., "Heat Distribution by Natural Convection: A Modeling Procedure for Enclosed Spaces," Master's Thesis, Dept. of Architecture, Massachusetts Institute of Technology, Cambridge, MA. (1978).

(7) Wray, W.O. and Weber, D.D., "LASL Similarity Studies, Part I," presented at 4th National Passive Solar Conference, Kansas City, Mo., 3-5 October 1979.

(8) Weber, D.D., Wray, W.O., Kearney, R, "LASL Similarity Studies, Part II," presented at 4th National Passive Solar Conference, Kansas City, Mo., 3-5 October 1979.

(9) Bauman, F., "Natural Convection in an Enclosure," Master's Thesis, Department of Mechanical Engineering, U.C. Berkeley, May 1979.

(10) Gadgil, A., Goldstein, D., Kammerud, R., and Mass, J., "Residential Building Simulation Model Comparison Using Several Building Energy Analysis Programs," presented at 4th National Passive Solar Conference, Kansas City, Mo., 3-5 October 1979.

(11) Raithby, G.D., Hollands, K.G.T., and Unny, T.E., "Analysis of Heat Transfer by Natural Convection Across Vertical Fluid Layers," J. Heat Transfer, Trans. ASME, 99, 287-293 (1977).

(12) MacGregor, R.K. and Emery, A.F., "Free Convection Through Vertical Plane Layers--Moderate and High Prandtl Number Fluids," J. Heat Transfer, Trans. ASME, 91, 392-401 (1969).

(13) Spalding, D.B., Int'l J. Numerical Methods in Engineering, 4, 551-559 (1972).

(14) Runchal, A.K., Int'l J. for Numerical Methods in Engineering, 4, 541-550 (1972).

(15) For a description of ADI and its application to fluid flow, see, e.g., Roache, P.J., Computational Fluid Dynamics, Hermossa Publishers, 1976.

(16) Patankar, S.V., in Studies in Convection, Vol 1, edited by B.E. Launder, Academic Press, 1975.

(17) Gadgil, A., "On Convective Heat Transfer in Building Energy Analysis," PhD Thesis, Dept. of Physics, U.C. Berkeley (November 1979).

(18) de Vahl Davis, G., "Laminar Natural Convection in an Enclosed Rectangular Cavity," Int'l J. Heat & Mass Transf., 11, 1675 (1968).

(19) Emery, A.F., J. Heat Transfer, (Trans. ASME), 11, 1675 (1963).

(20) Porter, J.J. and Arnas, O.A., Heat Transfer and Turbulent Buoyant Convection, Vol. II, Hemisphere Publishing Corp., 1977, pp. 797-806.

(21) Burnay, G., Hannay, J., and Portier, J., Heat Transfer and Turbulent Buoyant Convection, Vol. II, Hemisphere Publishing Corp., 1977, pp. 807-811.

(22) Rubel, A. and Landis, F., Phys. Fluids Suppl. II, 12, II-208 (1969).

(23) Fromm, J.E., "A Numerical Method for Computing the Nonlinear, Time Dependent, Buoyant Circulation of Air in Rooms," National Bureau of Standards Building Science Series, No. 39, 1971, pp. 451-464.

TABLE 1. COMPARISON OF HOT WALL $\overline{Nu}_{L_{IN}}$

RUN	Ra_L	EXPT'L	NUMERICAL	SURFACE TEMPS FOR NUMERICAL SIMULATIONS
1	2.4×10^9	79 ± 6	105	ESTIMATED FROM EXP'T
2a	4.7×10^{10}	165 ± 12	168	ESTIMATED FROM EXP'T
2b			201	HOT & TOP WALL = T_H COLD & BOTTOM WALL = T_C

FIG. 1. SCHEMATIC DIAGRAM

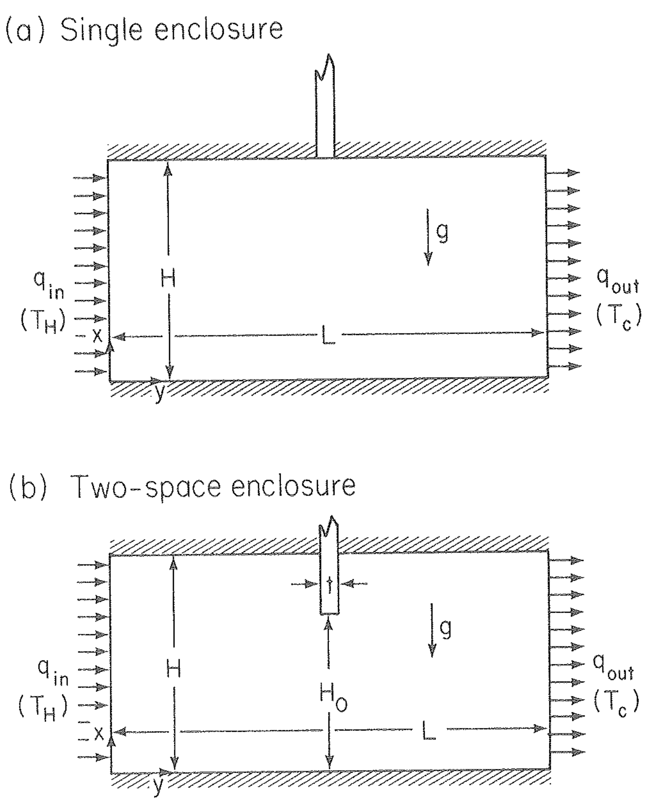

XBL 802-6623

FIG. 2. APPARATUS CROSS-SECTION

(1) - 1/2" Plexiglas
(2) - 3/16" Copper Sheet
(3) - Water
(4) - Thermofoil heaters
(5) - 3/8" O.D. copper tubing containing cooling water
(6) - High conductivity cement
(7) - 1/4" Plexiglas partition
(8) - Adjustable rod
(9) - 2" Polystyrofoam insulation board
(10) - Inside surface of polystyrofoam lined with polyethylene sheeting
(11) - Airspace
(12) - Thermocouple probe
(13) - Central Thermocouple array
(14) - Fiberglas insulation (2-layers)
(15) - Wood base

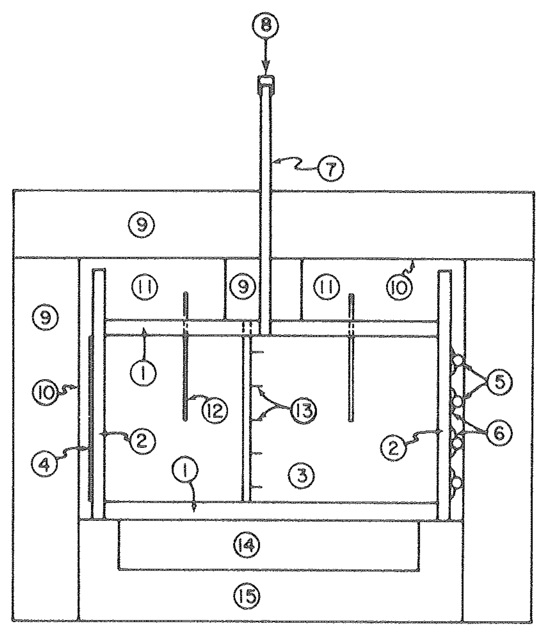

XBL 802-6634

FIG. 3. THERMOCOUPLE LOCATIONS (•)

① Copper plates
② Top of central opening
③ Bottom of central opening
④ Centerline vertical array
⑤ Thermocouple probes
⑥ Central partition temperature differential
⑦ Cooling water inlet
⑧ Cooling water outlet

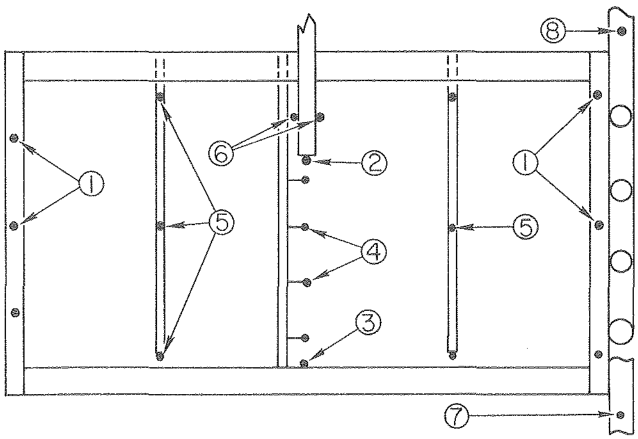

XBL 802·6624

FIG. 4. HEAT TRANSFER RESULTS AND COMPARISON

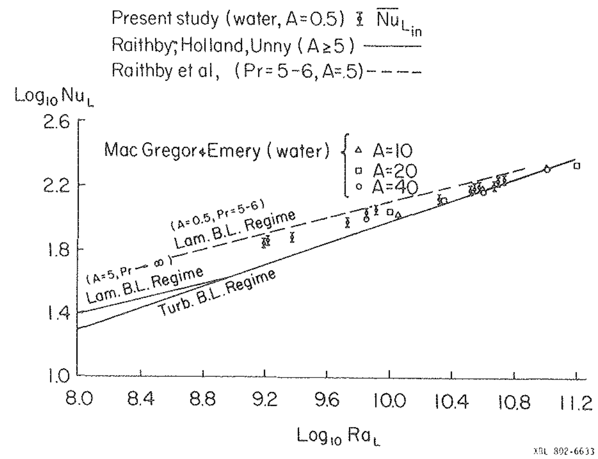

FIG. 5. HEAT TRANSFER RESULT, TWO-ZONE ENCLOSURE

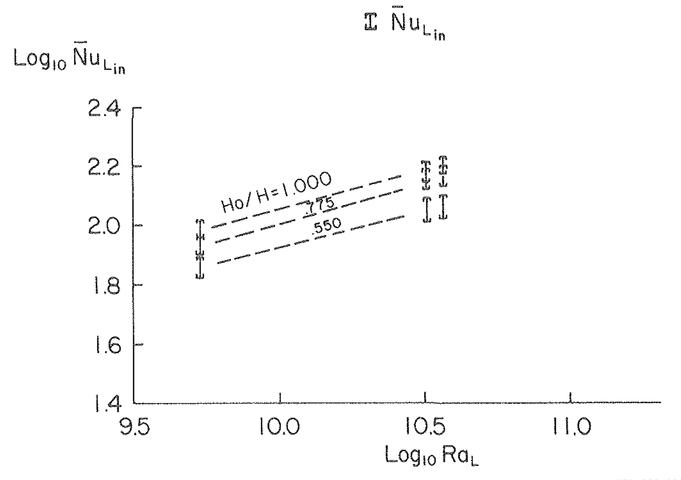

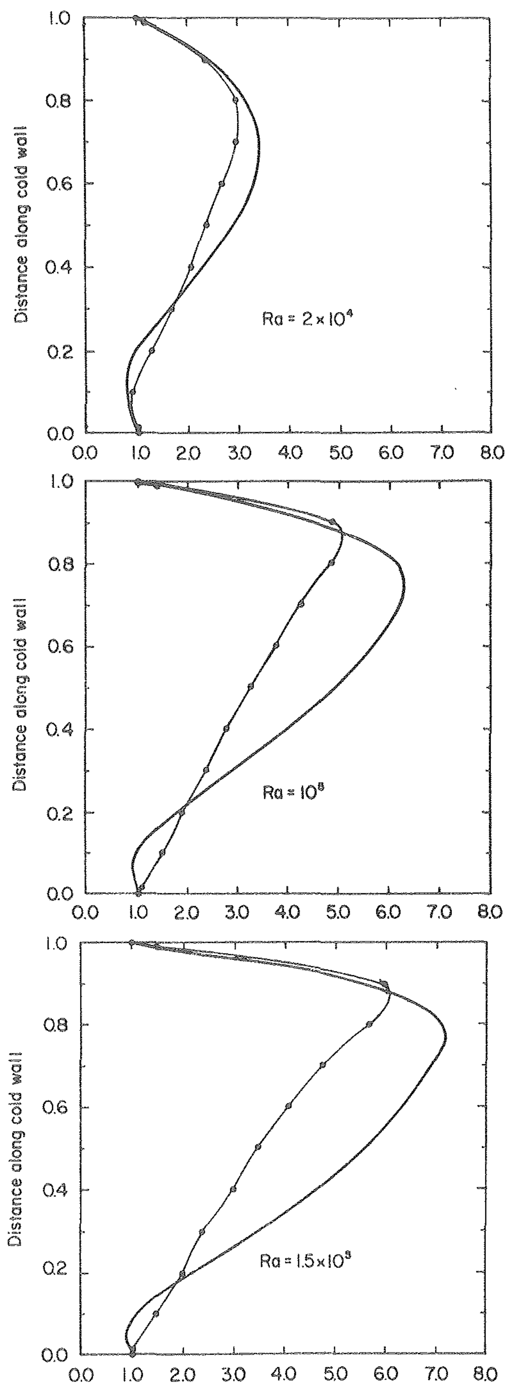

Local Nusselt Number

de Vahl Davis (1968) ————

Present Calculations -o-o-o-o-o-o-

FIGS. 6,7,8. Local Nusselt Number as a Function of Vertical Distance Along the Cold Wall of a Two-Dimensional Enclosure

FIG. 9. Dependence of $\overline{Nu}$ On Ra, for Two-Dimensional Flow Inside a Square Cavity. Comparison with Published Results.

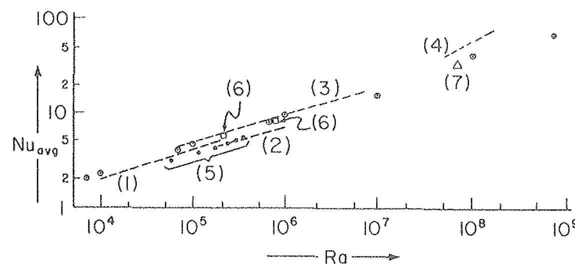

CURVE (1): DE VAHL DAVIS CALCULATIONS
CURVE (2): FROM RESULTS OF EMERY, EXPERIMENTAL
CURVE (3): PORTIER ET AL., CALCULATIONS, Pr = 0.7
CURVE (4): BURNAY ET AL., DATA REDUCED FROM EXPERIMENTS, Pr = 0.7
RESULTS (5) ARE OF RUBEL AND LANDIS, CALCULATIONS
RESULTS (6) ARE FROM QUON, CALCULATIONS
RESULT (7) IS FROM FROMM
POINTS INDICATED BY ⊙ ARE FROM PRESENT CALCULATIONS

FIG. 10. Schematic Diagram of Ruberg's Full-Scale Test.

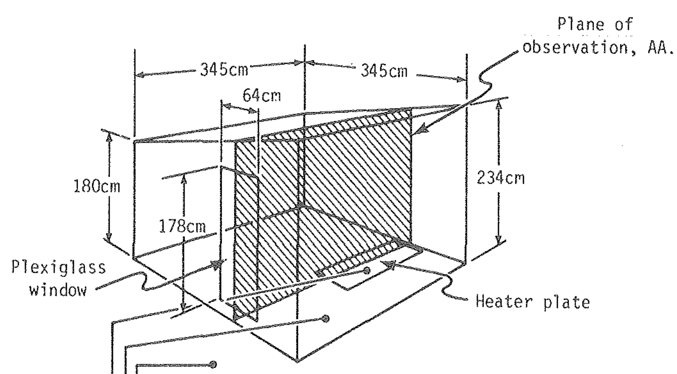

POSITION	C°	F°
Ambient air temperature	21.4	70.5
Room air temperature	40.6	105.1
Heater plate temperature	64.7	148.5

XBL7911-13133A

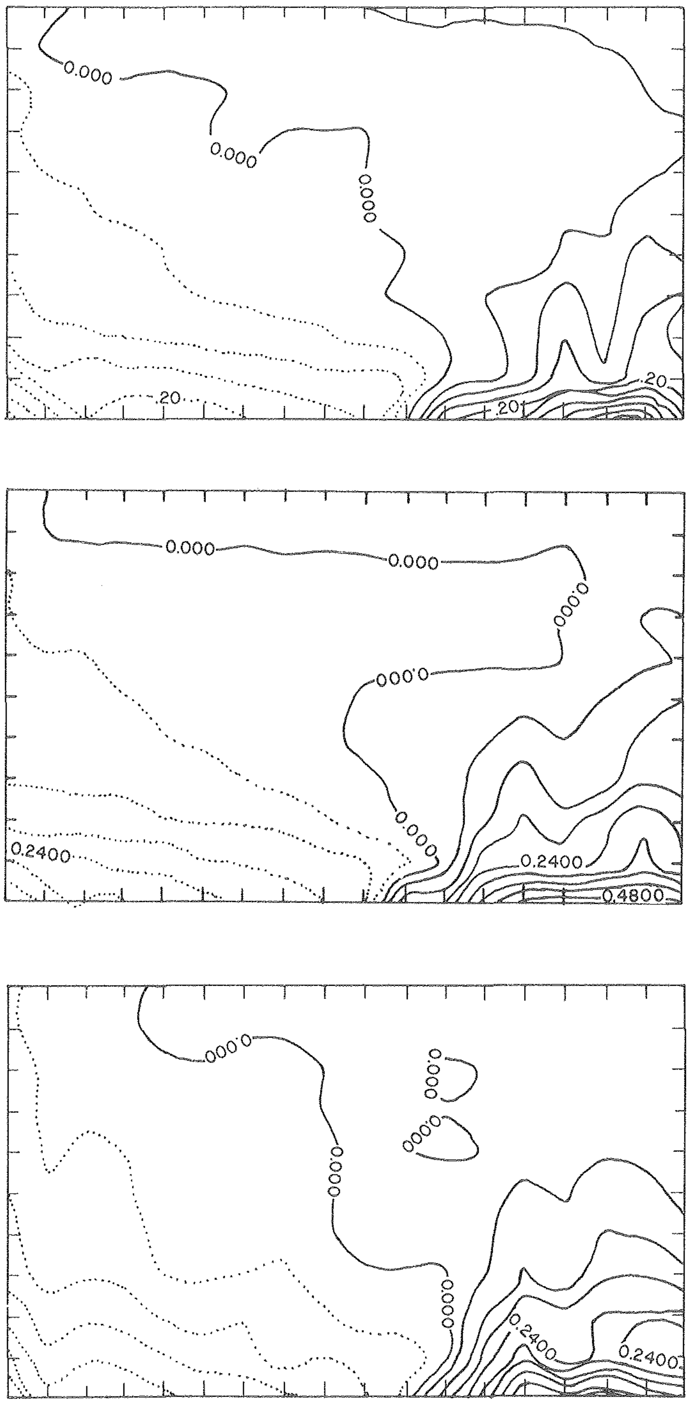

FIG. 11. Isotherms Measured in Ruberg's Experiments

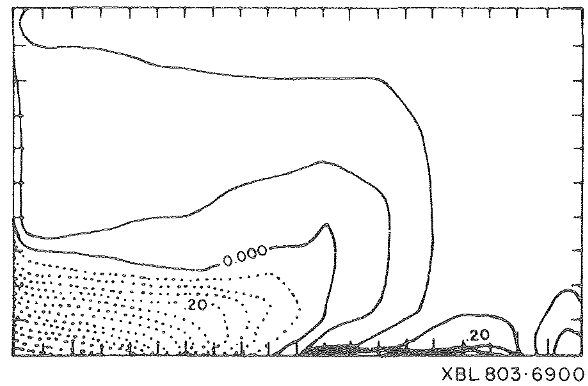

FIG. 12. Numerically Predicted Isotherms for Ruberg's Experiment

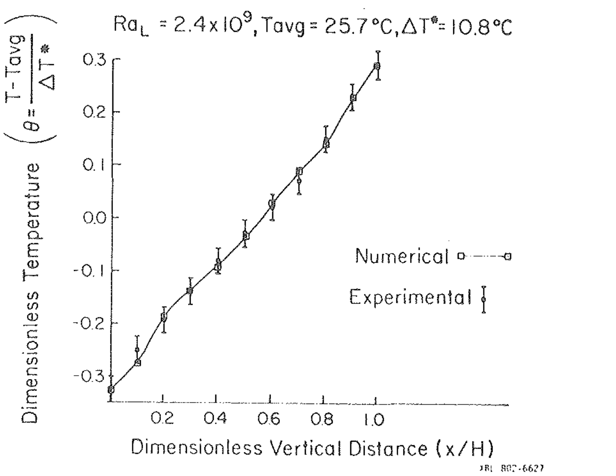

FIG. 13. Vertical Centerline (y/L=0.5) Temperature Profile

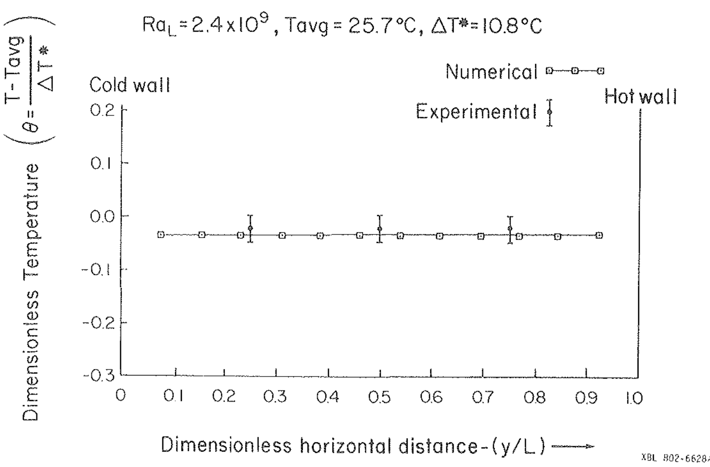

FIG. 14. Horizontal centerline (x/H=0.5) Temperature Profile

FIG. 15. Vertical Centerline (y/L=0.5) Temperature Profile

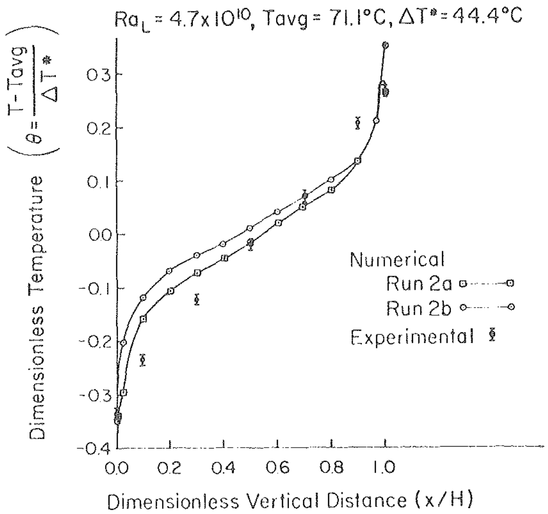

FIG. 16. Horizontal Centerline (x/H=0.5) Temperature Profile

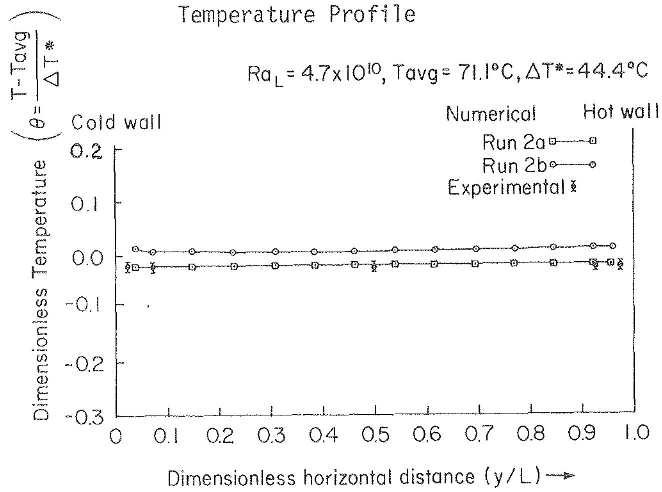

FIG. 17. Sensitivity of Convection Coefficients to Temperature Boundary Conditions

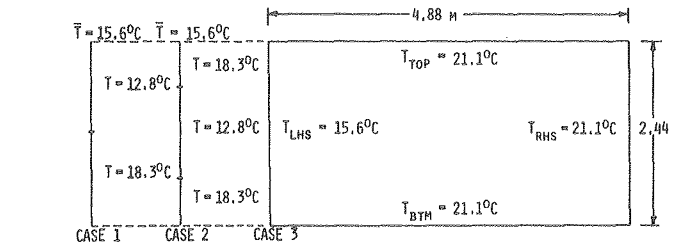

	Q/A (WATTS/M²)			
	LEFT HAND SIDE	BOTTOM	TOP	RIGHT-HAND SIDE
CASE 1	7.3	-3.9	-1.0	-2.5
CASE 2	7.5	-4.5	-0.4	-2.5
CASE 3	8.0	-5.0	-0.7	-2.4

FIG. 18. Nusselt Numbers for Different Surface Temperature Distributions

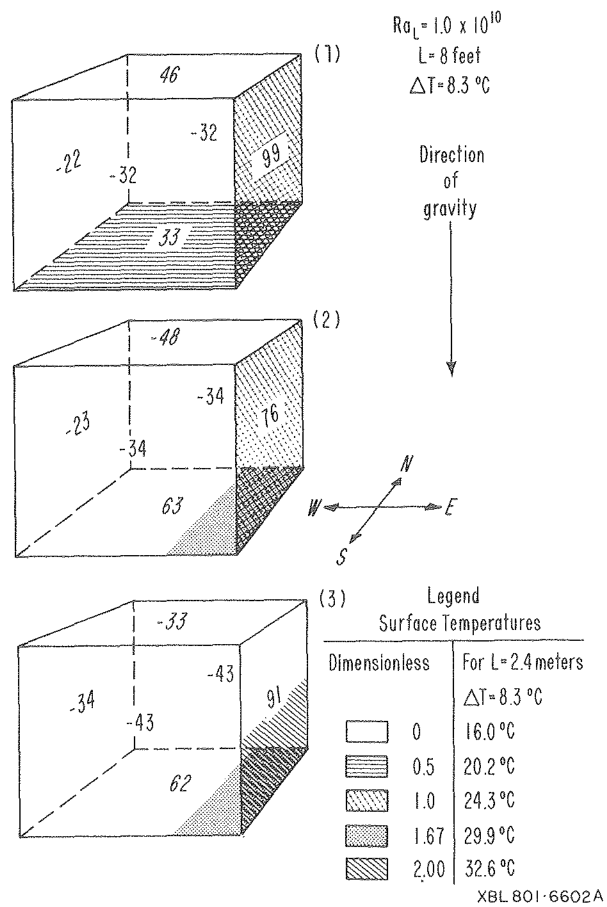

APPENDIX 1: NATURAL CONVECTION IN ENCLOSURES

A. Problem Definition

A prototypical problem in buoyancy-driven convection in an enclosure is shown schematically in Fig. A-1. The isothermal vertical walls in a two-dimensional cavity with adiabatic ceiling and floor surfaces are maintained at different temperatures, T_H and T_C. Recirculating flow is established due to the temperature-induced density variations in the working fluid.

Batchelor[1] was the first to describe the complex problem of the single enclosure and define the various flow regimes. He demonstrated that natural convection in a two-dimensional rectangular enclosure can be described completely by three independent dimensionless parameters:

(1) Aspect ratio, $A = H/L$

(2) Prandtl number, $Pr = \nu/\alpha$

(3) Rayleigh number, $Ra_L = Gr_L Pr = \frac{g\beta \Delta T L^3 Pr}{\nu^2}$

where ΔT and L establish temperature and length scales, respectively, for the problem. In the present work, the characteristic dimension, L, is taken to be the enclosure length, and the characteristic temperature difference, ΔT, is the temperature difference between the isothermal surfaces ($T_H - T_C$).

Defining the Rayleigh number based on the enclosure length (Ra_L) instead of the enclosure height (Ra_H) is done here for purposes of comparison to other studies. Ra_H would be a more meaningful choice, since heat transfer rates and transition to turbulence are dominated by the height of the vertical surfaces. The use of enclosure length (L) as the characteristic dimension tends to artificially increase the magnitude of the Rayleigh number ($Ra_L = 8Ra_H$ for $H/L = 0.5$) in enclosures of aspect ratio less than one.

The boundary conditions and fluid properties determine the nature of the recirculating flow. For low Rayleigh numbers, stable laminar flow is observed; as Ra_L increases, transition to turbulent flow can take place. The following discussion indicates that fully developed turbulence was not reached in the experimental runs reported here.

For a free-standing vertical plate of height H and at temperature, T_P, in a quiescent fluid at temperature, T_F, one can define a Rayleigh number, Ra'_H, based on the plate height and the temperature difference between the plate and the ambient fluid [$Ra'_H = g\beta(T_P - T_F)H^3Pr/\nu^2$]. It is commonly accepted that a turbulent boundary layer is established for $Ra'_H > 10^9$. In recirculating flow confined inside an enclosure, the horizontal surfaces of the enclosure will have a stabilizing influence which can delay the onset of turbulence by up to one order of magnitude in the Rayleigh number (10^{10}). Another factor of 2 must be included to take into account the difference in the definition of ΔT ($T_F = (T_H + T_C)/2$ for enclosure flow). It is therefore expected that transition to turbulence will occur for $Ra_H > 2 \times 10^{10}$; this translates to $Ra_L > 1.6 \times 10^{11}$ for the geometry ($A = 0.5$) of the present experiment.

B. Historical Perspective of Related Research

1. Heat Transfer Studies

Despite the large number of studies of natural convection in enclosures, a majority have been motivated by an interest in vertical air slots found in wall cavities or double-pane windows, and have therefore dealt with high aspect ratio ($A \geq 1$). The dimensions of most small-scale test facilities have limited the experimental results for air to the range $10^4 < Ra_L < 10^7$. Numerical studies, due to numerical instability at high Ra values, have also usually been restricted to boundary layer flow up to $Ra_L = 10^7$. In short, there has been little motivation or interest, and substantial difficulties, in approaching the problem of high Rayleigh number natural convection of air or other fluids in enclosures of aspect ratio slightly less than one (room-shaped geometries). A brief review of a few of the pertinent studies follows.

Elder[2,3] carried out extensive experimental studies in both the laminar and turbulent flow regimes using medicinal paraffin

---

[1]Batchelor, G.K., "Heat Transfer by Free Convection Across a Closed Cavity Between Vertical Boundaries at Different Temperatures," Quart. Appl. Math., 12, (3), 209-233 (1954).

[2]Elder, J.W., "Laminar Free Convection in a Vertical Slot," J. Fluid Mech., 23, 77-98 (1965).

[3]Elder, J.W., "Turbulent Free Convection in a Vertical Slot," J. Fluid Mech., 23, 99-111 (1965).

and silicone oil ($Pr \approx 10^3$). He presented some results for $A = 1$, but only in the laminar regime. An experimental and numerical study of moderate and high Prandtl number fluids was performed by MacGregor and Emery[4]. They presented some numerical results for $A = 1$ and $0.1 \leq Pr \leq 10$, but again limited to $10^4 \leq Ra_L \leq 10^5$. Their experimental data included results for water at large values of Ra_L ($Ra_L > 10^{10}$) with an aspect ratio of 10. Although limited to $A \geq 5$, Raithby et al.[5] use an approximate analysis to present some general heat transfer results covering $Pr > 0.71$ and all flow regimes (conduction, laminar, turbulent). Only three studies[6-8] (two experimental and one numerical) are reported in the aspect ratio range of 0.1 to 1.0. Sernas and Lee[8] discuss the importance of representative boundary conditions on the horizontal boundaries. Their results, however, are limited to a small range in the laminar flow regime ($1.9 \times 10^6 \leq Ra_L \leq 3.9 \times 10^6$).

2. Studies in Building Sciences

Past investigations of natural and forced convection within the building sciences have been motivated largely by a few specific situations in which these processes are known to be important. Among these, McCaffrey and Quintiere[9] have analyzed the role of natural convection between thermal zones as it affects the propagation of fires and the by-products of fires (e.g., smoke). Shaw[10,11] has experimentally investigated the convective mass transfer between rooms in hospitals in order to better understand the potential spread of contaminants. This investigation also attempted to evaluate the influence of the conventional air-handling system operation on the convective processes; however, since this study was performed in a specific room-diffuser configuration, one must question the applicability of these results to other configurations. Nielson[12] has performed numerical studies of convection driven by the room diffusers in conventional air systems. In these cases, the convection is driven by pressure gradients; the effect of buoyancy forces resulting from temperature differences is not significant.

APPENDIX 2: EXPERIMENTAL PROCEDURE

In this appendix, the procedures used in performing the natural convection experiment are described and the major sources of error are identified. The heaters and water flow rate were set to desired levels and the system was allowed to equilibrate (3-4 hours). Thermocouple readings were made individually over a period of about 15 minutes. The heat input rate (Q_{IN}) was read directly from three wattmeters; the heat output rate (Q_{OUT}) was obtained by measuring the cooling water inlet-to-outlet temperature differential and by timing and weighing the flow of cooling water.

---

[4] MacGregor, R.K. and Emery, A.F., "Free Convection Through Vertical Plane Layers--Moderate and High Prandtl Number Fluids," J. Heat Transfer, Trans. ASME, 91, 392-401 (1969).

[5] Raithby, G.D., Hollands, K.G.T., and Unny, T.E., "Analysis of Heat Transfer by Natural Convection Across Vertical Fluid Layers," J. Heat Transfer, Trans. ASME, 99, 287-293 (1977).

[6] Boyak, B.E. and Kearney, D.W., "Heat Transfer by Laminar Natural Convection in Low-Aspect Ratio Cavities," ASME Paper 72-HT-52, presented at the AIChE-ASME Heat Transfer Conf., Denver, Colo. (August 1972).

[7] Sernas, V., Fletcher, L.S., and Rago, C., "An Interferometric Study of Natural Convection in Rectangular Enclosure of Aspect Ratio Less Than One," ASME Paper 75-HT-63, presented at AIChE-ASME Heat Transfer Conference, San Francisco (August 1975).

[8] Sernas, V. and Lee, E.I., "Heat Transfer in Air Enclosures of Aspect Ratio Less than One," ASME Paper 78-WA/HT-7, presented at the ASME Winter Annual Meeting, San Francisco (December 1978).

[9] McCaffrey, B.J. and Quintiere, J.G., "Buoyancy Driven Countercurrent Flows Generated by a Fire Source," presented at Turbulent Buoyant Convection 1976 Int'l Centre for Heat and Mass Transfer, Dubrovnik, Yugoslavia, 30 August to 4 September 1976.

[10] Shaw, B.H., "Heat and Mass Transfer by Natural Convection and Combined Natural Convection and Forced Air Flow Through Large Rectangular Openings in a Vertical Partition," Proceedings, Int'l Mech. Engrg. Conference on Heat and Mass Transfer by Combined Forced and Natural Convection, Manchester, September 1971; vol. C.819, 31-39 (1972).

[11] Shaw, B.H. and Whyte, W., "Air Movement Through Doorways--The Influence of Temperature and Its Control by Forced Air Flow," Bldg. Serv. Engrg., 42, 210-218 (1974).

[12] Nielson, P.V., "Flow in Air Conditioned Rooms," Ph.D. Thesis, Technical University of Denmark (1974).

The thermocouple error ($\pm$ 0.5^{o}C) and the observed fluctuation error ($\mp$ 0.3^{o}C) due to incomplete mixing of outlet water resulted in some uncertainty in measuring the cooling water outlet temperature. The cooling water flow rate was kept low to produce sufficiently large values of ΔT_{CW} (in the range 3-8^{o}C), yielding a more accurate calculation of the heat removed through the cooled copper plate. This temperature difference introduced a horizontal temperature gradient on the cool plate of similar magnitude.

The method used for heating and cooling the copper plates resulted in nearly isothermal boundary conditions under small heat loads ($Ra_L < 10^{10}$); the maximum measured temperature variation across the surfaces of the heated and cooled plates were 1^{o}C and 2^{o}C, respectively. [This produces a characteristic error of $T_{var}/(T_H - T_C) \approx 25\%$.] However, for $Ra_L > 10^{10}$, large temperature stratification in the fluid combined with high rates of heat transfer to the vertical surfaces, resulting in a large vertical temperature gradient on each plate; the maximum variations on both plates were between 10-15^{o}C and $T_{var}/(T_H - T_C) \approx 45\%$.

For each experimental setting, average plate temperatures (T_H and T_C) were calculated and used in the evaluation of the characteristic Rayleigh number, Ra_L. Fluid properties were determined at the average temperature $T_{avg} = (T_H + T_C)/2$. Heat input and output values were used to find average Nusselt numbers for the hot plate ($Nu_{L_{IN}}$) and the cold plate ($Nu_{L_{OUT}}$):

$$\overline{Nu}_{L_{IN}} = \frac{Q_{IN}L}{kA_p\Delta T} \quad , \quad \overline{Nu}_{L_{OUT}} = \frac{Q_{OUT}L}{kA_p\Delta T}$$

The difference between these two Nusselt numbers was a measure of the heat losses from the insulated end walls and top and bottom surfaces.

Heat flux input q_{IN} ranged from 1100-20,200 W/m^2 and the plate temperature differential, $\Delta T = T_H - T_C$, ranged from 6-42^{o}C, yielding a corresponding Ra_L range of $1.6 \times 10^9 \leq Ra_L \leq 5.4 \times 10^{10}$. Cooling water flow rate varied from 0.27 to 3.7 liters/sec, resulting in $0^{o}C < \Delta T_{CW} < 8^{o}C$.

The main sources of error in this experiment were: (1) vertical surface temperature variations; (2) horizontal surface heat losses; (3) measurement of cooling water outlet temperature; and (4) measurement of average vertical surface temperatures from a few representative room surface temperature distributions.

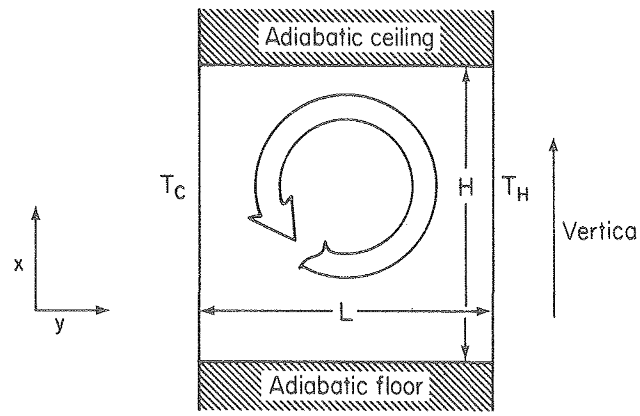

FIG. A-1. Recirculating flow induced in a fluid inside a two-dimensional square cavity, defined by adiabatic floor and ceiling and isothermal walls, at temperatures T_H and T_C ($T_H > T_C$).